Effects of Extrusion Conditions on Rheological Behavior of Acrylonitrile–Butadiene–Styrene Terpolymer Melt

JI-ZHAO LIANG*

Department of Industrial Equipment and Control Engineering, South China University of Technology, Guangzhou 510641, People's Republic of China

Received 21 February 2001; accepted 9 October 2001

ABSTRACT: The influence of temperatures and flow rates on the rheological behavior during extrusion of acrylonitrile–butadiene–styrene (ABS) terpolymer melt was investigated by using a Rosand capillary rheometer. It was found that the wall shear stress (τ_w) increased nonlinearly with increasing apparent shear rates and the slope of the curves changed suddenly at a shear rate of about 10^3 s^{-1}, whereas the melt-shear viscosity decreased quickly at a τ_w of about 200 kPa. When the temperature was fixed, the entry-pressure drop and extensional stress increased nonlinearly with increasing τ_w, whereas it decreased with a rise of temperature at a constant level of τ_w. The relationship between the melt-shear viscosity and temperature was consistent with an Arrhenius expression. The results showed that the effects of extrusion operation conditions on the rheological behavior of the ABS resin melt were significant and were attributable to the change of morphology of the rubber phase over a wide range of shear rates. © 2002 Wiley Periodicals, Inc. J Appl Polym Sci 85: 606–611, 2002

Key words: acrylonitrile–butadiene–styrene (ABS) terpolymer; melt extrusion; flow property; entry-pressure losses; extensional viscosity

INTRODUCTION

Acrylonitrile–butadiene–styrene terpolymer (ABS) is an engineering plastic used widely in industry because of its good mechanical and processing properties. ABS is usually filled with rubber particles[1] or rigid inorganic particles (RIP), such as calcium carbonate ($CaCO_3$),[2] kaolin, and glass bead,[3] and talcum powder,[4] to further enhance its strength, toughness, and stiffness as well as to reduce the production cost. In the recent two decades, the mechanical properties of ABS, its blends, and composites have been intensively studied.[3–10] The results showed that the tensile strength of ABS/RIP composites decreased with the increase of the filler content.[4,5] Turcsanyi et al.[5] studied the relationship between tensile yield stress and the interfacial adhesion between the matrix and fillers, and proposed a general expression containing a constant B, to distinguish the type of the interfacial bonding: poor ($B < 3$), good ($B \approx 3$), or strong ($B > 3$). They found that the interfacial adhesion between the ABS matrix and glass beads was poor whenever the filler surface was pretreated, that is, when $B = 0.25$–1.1.

The melt rheological behavior plays an important role both in polymer processing and shaping, and in design of machinery used in processing. Thus, the viscoelastic properties of ABS melt have been the focus of intense interest in the last decade, in such areas as the effects of processing conditions on the phase morphology and the melt-welding strength,[10–12] the effects of viscosity ratio on the morphology and mechanical properties,[13] the melt-shear viscosity,[14] and viscoelastic-

* E-mail: scutjzl@263.net.

Journal of Applied Polymer Science, Vol. 85, 606–611 (2002)

ity.[15] In the previous work,[2] Tang and Liang investigated the effects of the filler content, size, and its surface treatment on the melt-flow behavior of ABS/$CaCO_3$ composites. However, there have been relatively few studies on melt rheology of ABS resin under a wide range of extrusion flow rates and temperatures. The objectives of this investigation are to measure the melt rheological properties, such as entry-pressure losses, extensional stress, and viscosity in capillary extrusion of an ABS resin at high shear rates.

EXPERIMENTAL

Materials

The resin used as the matrix in this test was Polytac ABS PA757, an extrusion-grade resin supplied by Chi Mei Co. (Taibei, Taiwan, China). The solid-state density and melt flow rate of the resin were 1.05 g/cm^3 and 1.5 g/10 min (ASTM D1238), respectively.

Apparatus and Methodology

An off-line twin-bore capillary rheometer (Rosand Precision RH7) was used in these tests. The bore–die contraction ratio was 15 : 1 and the entrance angle was 180°. One die was 1 mm in diameter and 16 mm long; the other had the same diameter but had an effectively zero length (i.e., an orifice die), giving an entrance-pressure drop by extrapolation and the Rabinowitsch correction to obtain the true shear rate.

The rheological properties of the resin melt, such as entry-pressure losses, extensional and shear stresses, and shear and extensional viscosity, were measured at a temperature range of 200–240°C and a wide apparent shear rate varied from 10 to 10^4 s^{-1}. In this case, the shear stress at the channel wall (τ_w) is defined as

$$\tau_w = \frac{(\Delta P - \Delta P_{en})D}{4L} \tag{1}$$

where ΔP is the total pressure in the long capillary extrusion of the melt, and L and D are the die length and diameter, respectively.

The apparent shear rate $\dot{\gamma}_a$ is defined as

$$\dot{\gamma}_a = \frac{32Q}{\pi D^3} \tag{2}$$

According to the shear rate correction method of Rabinowitsch, the true shear rate $\dot{\gamma}_w$ is given by

$$\dot{\gamma}_w = \frac{3n + 1}{4n}\,\dot{\gamma}_a \tag{3}$$

Thus the true melt-shear viscosity can be expressed as

$$\eta_s = \tau_w/\dot{\gamma}_w \tag{4}$$

RESULTS AND DISCUSSION

Entry Flow

Polymer melts undergo significant entry-pressure losses upon entering a small or narrow flow channel from a large flow section, which is characterized by entry-pressure drop (ΔP_{en}). This entry-pressure drop has been ascribed to both shear and elongation flow.[16] Therefore, the main factors affecting ΔP_{en} during extrusion of polymer melt are temperature, extrusion rate, and channel geometry (e.g., conduct contraction ratio). Based on the flow analysis of the second-order fluid in a conic die by using the tensor method and the following suppositions: (1) the melt is incompressible and isothermal in the die flow; (2) the influence of gravity and inertia on the flow can be neglected, given the high viscosity and low velocity of the melt; and (3) there is no slip phenomenon at the die wall and flow presents a radial character, Liang et al.[17] proposed an expression for prediction of ΔP_{en} as follows:

$$\Delta P_{en} = 2K_E \ln Z(2K_s\dot{\gamma}_w^n + \tfrac{1}{2}K_E K_e \dot{\gamma}_w^m) + K_s\dot{\gamma}_w^n[1 - (1/Z)^{3n}]/3nK_E \tag{5}$$

where K_s and n are the power index constants for shear flow; K_e and m are the power index constants for elongation flow; Z is the channel-contraction ratio ($Z = D_R/D$, where D_R is the reservoir diameters); and K_E is a function of the half natural entry converging angle (θ_0) of viscoelastic fluids, which is given by:

$$K_E = \tfrac{1}{2}\tan\theta_0 \tag{6}$$

Figure 1 shows the dependency of the ΔP_{en} measured from the sample experiments on shear stress at the channel wall (τ_w) of the melt at

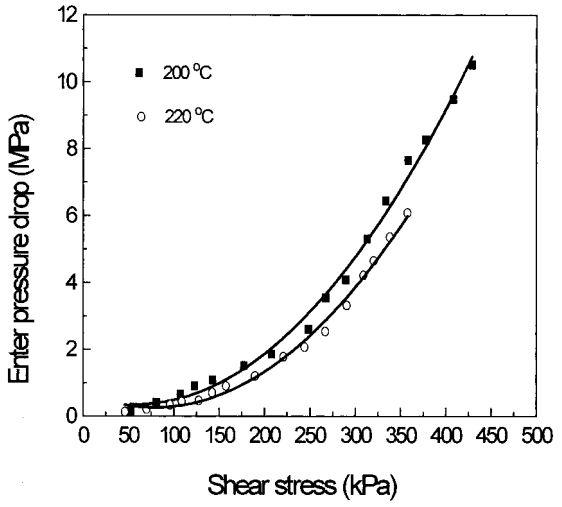

Figure 1 Entrance-pressure drop as a function of shear stress.

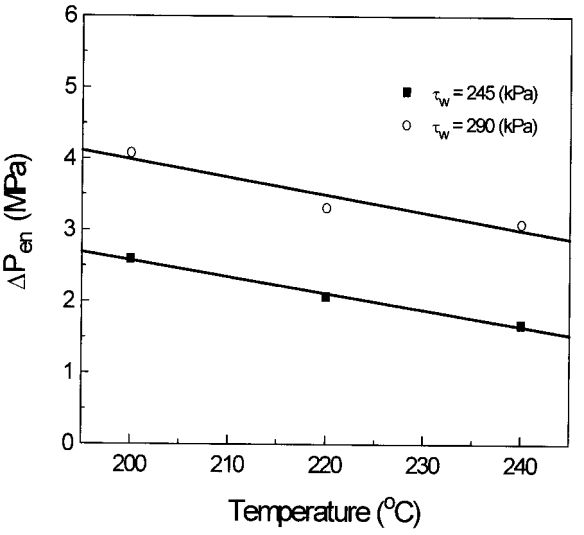

Figure 2 Dependency of entrance-pressure drop on temperature.

constant temperature. It can be seen that ΔP_{en} increases nonlinearly with the increase of τ_w, and decreases with a rise of temperature. When the test temperature is fixed, shear stress or shear rate at the channel wall increases with the increase of extrusion rate, and the converging flow is concomitantly enhanced. In this case, the elongation and shear deformation are increased and the elastic and plastic deformation energies stored in the melt are correspondingly increased during the die entrance flow, resulting in the addition of entry-pressure losses. In eq. (5), the terms $K_s\dot{\gamma}_w^n$ and $K_e\dot{\gamma}_w^m$ represent, respectively, shear stress and extensional stress, if in fact, the fluid flow at the die inlet obeys the power law.

Figure 2 illustrates the influence of the test temperature on ΔP_{en} for the sample melt. At a constant level of τ_w, ΔP_{en} decreases approximately linearly with an increase of temperature. When the extrusion rate is fixed, the motion ability of macromolecular chains is enhanced with a rise of temperature, and the melt-shear viscosity and elongation viscosity decrease correspondingly, leading to reduction of the extension deformation energy dissipations and entry-pressure drop.

Shear-Flow Properties

The flow curve is an important characterization for the processing properties of polymer melts under technological conditions. It is usually represented by the relationship between τ_w and apparent shear rate $\dot{\gamma}_a$ for die extrusion of polymer materials. Figure 3 displays the relationship between τ_w and $\dot{\gamma}_a$ for the sample melts at different test temperatures. It can be seen that τ_w increases nonlinearly with increasing $\dot{\gamma}_a$ in a bilogarithmic system when the test temperature is constant. This suggests that the melt-shear flow does not obey Hooke's law in this case.

Figure 4 illustrates the relationship between the melt-shear viscosity η_s for the sample melt and shear stress at a constant test temperature. It can be seen that η_s decreases relatively gradually when $\tau_w \leq 200$ kPa, whereas it decreases quickly when $\tau_w \geq 200$ kPa at 200°C. In other words, the change in slope of the $\eta_s - \tau_w$ curve

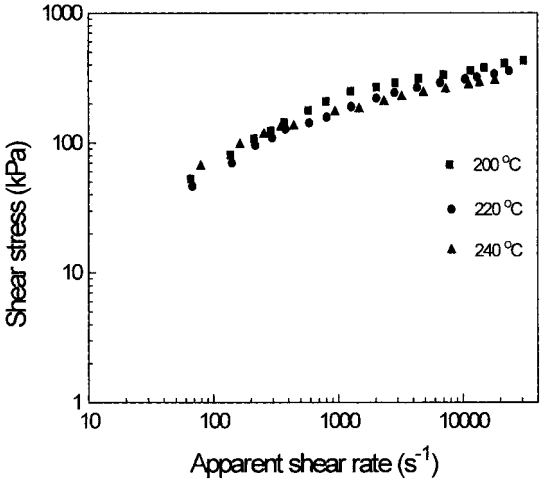

Figure 3 Shear stress versus apparent shear rate.

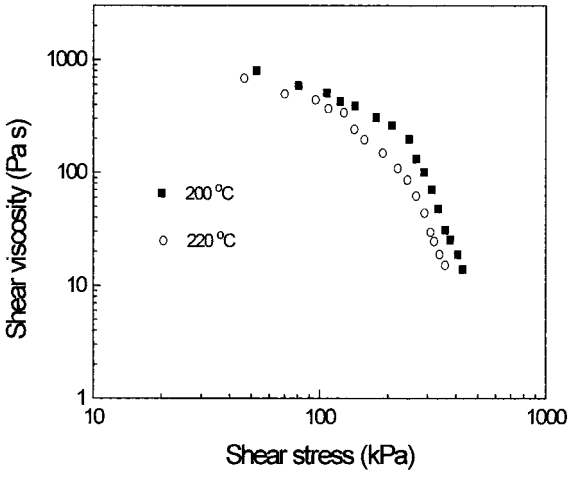

Figure 4 Shear viscosity versus shear stress.

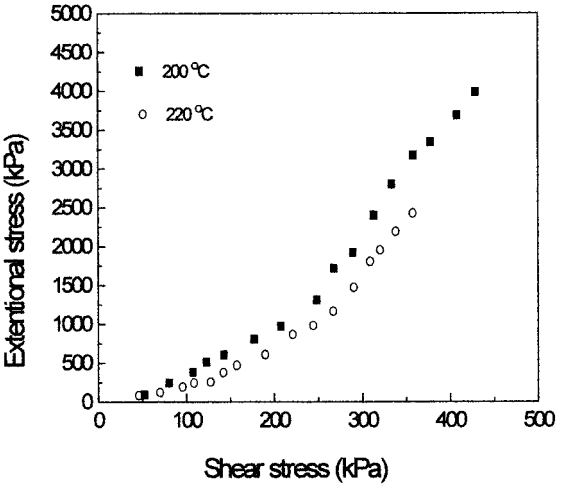

Figure 6 Dependency of extensional stress on shear stress.

appears obvious in this case. Furthermore, η_s also decreases nonlinearly with the increase of τ_w in a bilogarithmic system.

Figure 5 shows the dependency of η_s for the sample melt at the test temperature. At a constant level of τ_w, ln η_s increases linearly with the reciprocal of the absolute temperature ($1/T$). This means that the dependency of the melt-shear viscosity is consistent with an Arrhenius expression, given by

$$\eta_S = \eta_0 \exp\left(\frac{E_s}{RT}\right) \tag{7}$$

where η_0 is the viscosity coefficient, E_s is the activation energy in viscous flow, and R is the universal gas constant. In addition, it can be also seen in Figure 5 that the slope of the ln η_s − $1/T$ curve at τ_w = 290 kPa is greater than that at τ_w = 245 kPa. This indicates that the sensitivity of the melt-shear viscosity to temperature somewhat increases with the addition of shear stress.

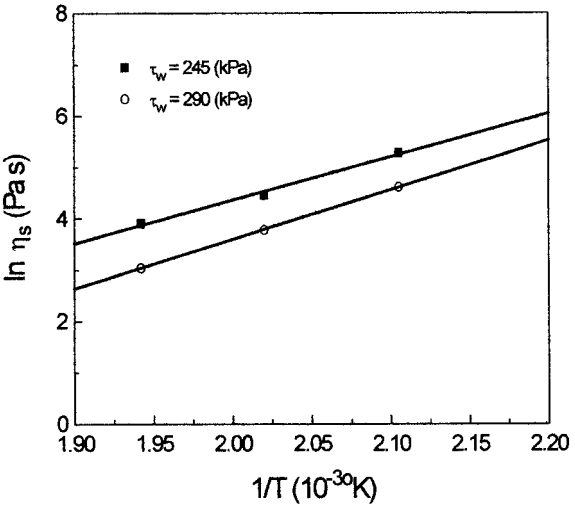

Figure 5 Dependency of shear viscosity on temperature.

Extensional Flow Properties

As stated above, polymer melt flow at the entrance of the duct includes shear flow and extensional flow. Extensional stress (σ_t) and extensional viscosity (η_e) are the important parameters for characterization of extensional flow properties of viscoelastic fluids. Cogswell[16] presented simplified expressions for estimation of σ_t and η_e for flow in conicocylindrical dies as follows:

$$\sigma_t = \tfrac{3}{8}(n + 1)\Delta P_{en} \tag{8}$$

and

$$\eta_e = \frac{9(n + 1)^2}{32\eta_s}\left(\frac{\Delta P_{en}}{\dot{\gamma}_w}\right)^2 \tag{9}$$

In this study, the values of σ_e and η_e in extrusion of the sample melt were estimated by using eqs. (8) and (9). Figure 6 shows the correlation between extensional stress and shear stress for the sample melt. When the test temperature is fixed, σ_t increases nonlinearly with increasing τ_w, whereas it decreases with a rise of temperature. As noted above, ΔP_{en} increases nonlinearly with the addition of extrusion rates. Furthermore, the

melt-flow behavior index (n) also increases somewhat correspondingly with increasing extrusion rates, resulting in an increase of extensional rates at the inlet. Consequently, σ_t increases concomitantly in this case [see eq. (8)].

Figure 7 displays the dependency of σ_t on temperature at a constant level of shear stress. It can be seen that σ_t decreases linearly with a rise of temperature, whereas it increases with an increase in the level of shear stress. For a given polymer and duct contraction ratio Z [see eq. (5)], the elastic deformation energy stored in the melt entry flow decreases because of the reduction of melt viscosity with an increase of temperature, and the entry-pressure losses decrease accordingly, leading to a decrease of extensional stress. Figure 8 shows the effect of test temperature on the melt extensional viscosity at different levels of shear stress. Similarly, the melt extensional viscosity decreases linearly with a rise of temperature, whereas it increases with the increase of the level of shear stress. In general, the motion ability of macromolecular trains of polymer materials is enhanced with a rise of temperature, and the resistance between molecular chains decreases and entry-pressure losses decline, leading to reduction of the melt-shear viscosity and extensional viscosity [see eq. (9)].

In general, the rheological properties depend greatly on the morphology of components for polymer alloys or polyblends in the rubber phase. ABS is a two-phase system in which styrene–acrylonitrile copolymer (SAN) is the continued phase and butadiene rubber is the dispersed phase. Thus,

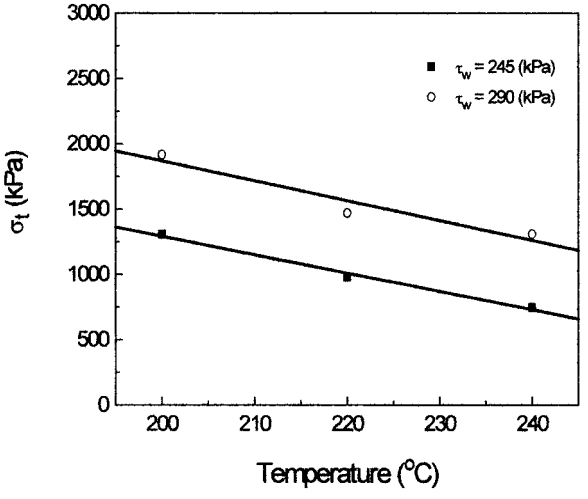

Figure 7 Extensional stress as a function of temperature.

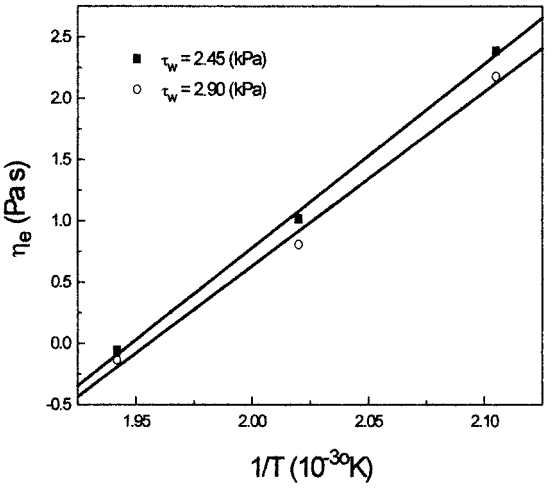

Figure 8 Extensional viscosity as a function of temperature.

the rheological properties of ABS resin melt are significantly related to the morphology of the rubber phase. For example, the difference in rheological properties, such as melt viscosity, end-pressure losses, and die–swell behavior, between the one-phase continuous structure (e.g., "see-island" structure) and the two-phase continuous structure (e.g., laminar structure) is obvious. Apart from the rubber phase composition, the particle size, and its distribution, processing conditions affect, to some extent, the interfacial morphology between phases. For instance, shear or elongation will induce crystallization resulting from macromolecular chain orientation during die extrusion flow of crystalline polymer at certain temperatures, leading to a change of entry-pressure losses.[18] When the test temperature is fixed, the smaller deformation of rubber particles is produced, and the interfacial morphology is a "see-island" continuous structure at lower shear stress level, resulting in decreasing viscosity relatively slightly with increasing shear stress. At higher shear stress level, a larger deformation of rubber particles is propagated, and the interfacial morphology is a laminar continuous structure; the flow resistance between the melt layers reduces concomitantly, leading to a rapid decrease in viscosity with increasing shear stress (Fig. 4).

CONCLUSIONS

When the temperature was fixed, the slopes of the flow curves of the ABS melt changed suddenly at

a shear rate of about 10^3 s^{-1}, suggesting that the melt-flow behavior of the sample in the lower shear rate range is different from that in the high shear rate range. Similarly, the shear viscosity decreased quickly at a shear stress of about 200 kPa.

The entry-pressure drop and extensional stress increased nonlinearly with increasing τ_w, whereas it decreased linearly with a rise of temperature at constant τ_w. The shear and extensional viscosities decreased with an increase of temperature at a constant level of τ_w, and the relationship between them was consistent with an Arrhenius expression. The results showed that the effects of extrusion operation conditions on the melt rheological behavior were significant.

The authors thank T. L. Wong of the Hong Kong Plastic Technology Center for his help in the experiments.

REFERENCES

1. Grancio, M. R. Polym Eng Sci 1972, 12, 213.
2. Tang, C. Y.; Liang, J. Z. in Proceedings of the IMCC 2000, Hong Kong, August 16–17, 2000; pp 45–46.
3. Lavengood, R. E.; Nicolais, L.; Narkis, M. Appl Polym Sci 1973, 17, 1173.
4. Bigg, D. M. Polym Compos 1987, 8, 115.
5. Turcsanyi, B.; Pukanszky, B.; Tudos, F. J Mater Sci Lett 1988, 7, 160.
6. Narkis, M. J Appl Polym Sci 1976, 20, 1597.
7. Newmann, L. V.; Williams, J. G. J Mater Sci 1980, 15, 773.
8. Lu, M.-L.; Lee, C.-B.; Chang, F.-C. Polym Eng Sci 1995, 35, 1433.
9. Yang, K.; Lee, S.-H.; Oh, J.-M. Polym Eng Sci 1999, 39, 1667.
10. Selden, R. Polym Eng Sci 1997, 37, 205.
11. Stokes, V. K. Polym Eng Sci 1997, 37, 692.
12. Chaudhry, B. I.; Hage, E.; Pessan, L. A. J Appl Polym Sci 1998, 67, 1605.
13. Yang, K.; Lee, S.-H.; Oh, J.-M. Polym Eng Sci 1999, 39, 1667.
14. Araki, T.; White, J. L. Polym Eng Sci 1998, 38, 590.
15. Bertin, M.-P.; Marin, G.; Montfort, T.-P. Polym Eng Sci 1995, 35, 1394.
16. Cogswell, F. N. Polym Eng Sci 1972, 12, 64.
17. Liang, J. Z. J Appl Polym Sci 2001, 80, 1150.
18. Ness, J. N.; Liang, J. Z. J Appl Polym Sci 1993, 48, 557.